Nat. Hazards Earth Syst. Sci., 13, 709–719, 2013
www.nat-hazards-earth-syst-sci.net/13/709/2013/
doi:10.5194/nhess-13-709-2013

Natural Hazards and Earth System Sciences
Open Access

The 20 February 2010 Madeira Island flash-floods: VHR satellite imagery processing in support of landslide inventory and sediment budget assessment

C. Lira[1], M. Lousada[1], A. P. Falcão[2], A. B. Gonçalves[2], S. Heleno[1], M. Matias[1], M. J. Pereira[1], P. Pina[1], A. J. Sousa[1], R. Oliveira[3], and A. B. Almeida[3]

[1]CERENA – Centre for Natural Resources and the Environment, Instituto Superior Técnico, Universidade Técnica de Lisboa, Lisbon, Portugal
[2]ICIST – Instituto de Engenharia de Estruturas, Território e Construção, Instituto Superior Técnico, Universidade Técnica de Lisboa, Lisbon, Portugal
[3]CEHIDRO – Centre for Hydrosystems research, Instituto Superior Técnico, Universidade Técnica de Lisboa, Lisbon, Portugal

Correspondence to: A. J. Sousa (ajsousa@ist.utl.pt)

Received: 12 July 2012 – Published in Nat. Hazards Earth Syst. Sci. Discuss.: –
Revised: 9 January 2013 – Accepted: 28 January 2013 – Published: 20 March 2013

Abstract. On 20 February 2010, an extreme rainfall episode occurred on Madeira Island, which caused an exceptionally strong flash flood and several soil slip-debris flows, producing 45 confirmed deaths and 6 persons declared missing, as well as extensive material damages. In order to understand and quantify the importance of landsliding in routing sediment through mountainous drainage, such as Madeira Island's landscape, it was essential to perform extensive landslide analysis. This study describes the methodology used to semi-automatically detect the landslides, produce the landslide inventory maps and estimate the sediment volume produced during this particular event which ranged from 217 000 m^3 to 344 000 m^3 and 605 000 m^3 to 984 000 m^3 for the Funchal and Ribeira Brava basins, respectively. These results contributed to the design and implementation of measures to prevent damages caused by landslides in Madeira Island.

1 Introduction

Madeira Island (Fig. 1) has a long record of flash floods, and since the beginning of the 19th century at least 30 flash flood events of significant intensity were registered (SRA/INAG, 2003; Almeida et al., 2010). The flash flood, locally named "aluvião" is a phenomena characterized by the flow of a large amount of sediment transported by water, concentrated in a small period of time (few hours), which can be extremely damaging. The trigger mechanism is usually a heavy rain episode that floods the river courses and their banks, and allows the accumulated sediments to be transported downstream very quickly and with enormous energy. These flash floods are associated with the formation of landslides (Rodrigues and Ayala-Carcedo, 2000, 2003a, b; Almeida et al., 2010), that usually nourish the torrential flow with sediments and that per se produce damages and sometimes even human casualties. The occurrence of landslides on Madeira Island is very common because of the combination of steep slopes (37 % of mean slope angle) with episodes of heavy rain associated with a subtropical climate (Guzzetti et al., 2004; Aleotti, 2004; Giannecchini, 2006; Lira et al., 2011a). The risk associated with the occurrence of this type of phenomena is very high in Madeira, due to the large population (247 k inhabitants) with 50 % of its total population concentrated in the municipality of Funchal and 93 % on the south side of the island (including Funchal).

The landslides of 20 February 2010 in Madeira were caused by a flash flood event, here after referred as the 2010 event; this was a particularly extreme phenomenon because it results from the combination of an extreme rainfall event and a long-lasting rainfall period (Fragoso et al.,

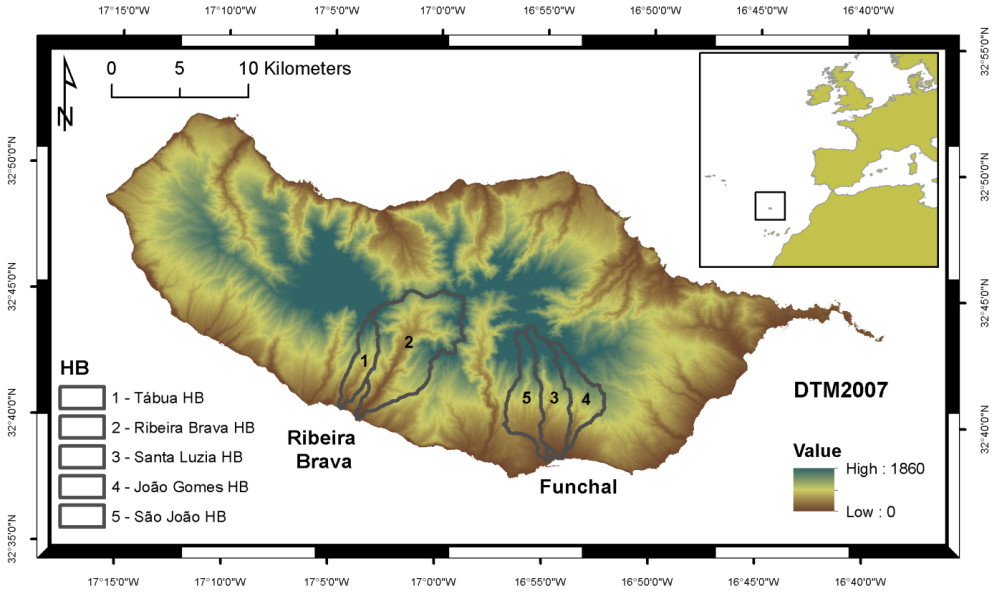

Fig. 1. Location of Madeira Island on the North Atlantic (top right) and Digital Terrain Model (DTM) of the island. The most affected basins during the 2010 event are delimited.

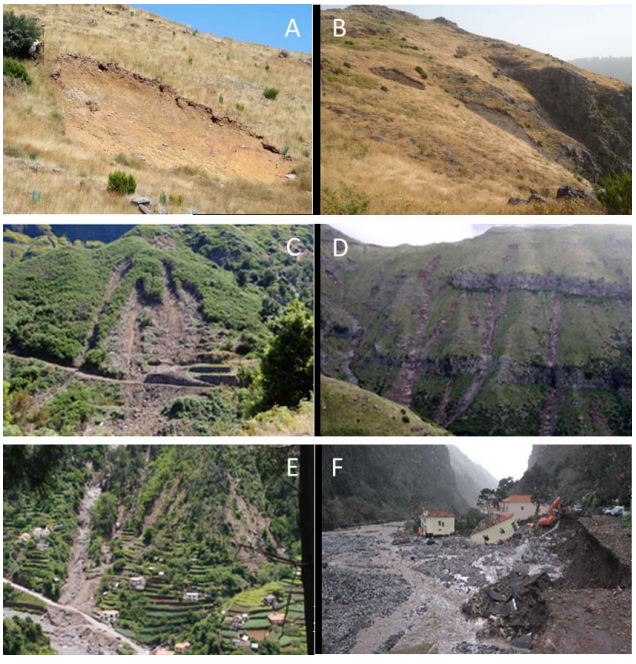

Fig. 2. Shallow landslides trigged during the 2010 event: **(A)** and **(B)** – soil-slips; **(C)**, **(D)**, and **(E)** – soil slip-debris flows; **(F)** – material damages.

2012). These conditions caused an exceptionally strong flash flood and several soil slip-debris flows, according to Cruden and Varnes (1996) terminology, affecting most severely the municipalities of Funchal and Ribeira Brava. Rainfall values reached more than the double of the monthly average: between 06:00 a.m. LT (local time) and 11:00 a.m. LT of the above mentioned day, 108 mm were registered at Funchal station and 146 mm at Pico do Areeiro station. In casualties, the flash flood and landslides were responsible for 45 deaths, 250 injured and 600 homeless persons, and also caused severe economic damage. Ribeira Brava town, as well as most parts of downtown Funchal, were completely flooded (Fig. 2).

In the aftermath of the event, the local governmental authorities decided to establish principles and strategies to cope with future cases (Almeida et al., 2010). To contribute to that goal, a broad team of experts conducted several studies to characterise this extreme event: some members dealt with the description of the precipitation, others with the geological, geotechnical and hydraulic aspects, while others dealt with the landslides itself.

The principal objective of the present study is to describe the methodology used to semi-automatically detect the landslides, produce a complete landslide inventory map, and estimate the sediment volume produced during the 2010 event. This description was essential to understand and quantify the importance of landsliding in routing sediment through mountainous drainage, such as Madeira landscape; and to assist the support decisions and the design of the mitigation interventions, such as the construction of physical barriers capable of retaining the sediments.

2 Background

Recent developments have taken place in the use of remote sensing techniques and image analysis to evaluate the extension and impact damages of landslides (Fernández et al.,

2005; Nichol and Wong, 2005; Danneels et al., 2007; Liu et al., 2009; Martha et al., 2010). Landslide inventory mapping can also greatly improve from the use of these techniques (Whitworth et al., 2003; Malamud et al., 2004; Kirschbaum et al., 2009). Depending on the type of landslides, different approaches can be adopted (Whitworth et al., 2001, 2005). Bucknam et al. (2001), Cardinali et al. (2001) and Guzzetti et al. (2004) use aerial photographs taken shortly after the event and stereoscopic techniques to interpret the phenomenon and produce an inventory landslides map. McKeana and Roering (2004), Ardizzone et al. (2007), Corsini et al. (2007), Schulz (2007), Van Den Eeckhaut et al. (2007) and Kasai et al. (2009) use digital analysis of high resolution DEMs. With the dissemination and the increasing usage of very high resolution (VHR) satellite panchromatic images (e.g. QuickBird, Ikonos, WorldView-1 and 2, GeoEye-1) the detection of landslides has the potential to be more exhaustive and has reached a sub-meter precision, allowing more accurate sediment budget calculations (Dong et al., 2009). This fact is essential when one deals with numerous small landslides affecting wide areas, making the inventory very difficult to perform without the use of these VHR images. The use of an automated methodology to detect and identify such features is essential; otherwise the task would be extremely time-consuming.

One of the main applications of mapping landslide events is the assessment of the displaced volume of sediments produced during the occurrence of the phenomena. The quantification of landslide volume is important to determine landslide susceptibility and hazard (Guzzetti et al., 2009), and also to support post-event mitigation actions, such as sediment control measures (Galiatsatos et al., 2007; Takara et al., 2010). Although crucial, the determination of landslide volume is not as straightforward as the quantification of the number of landslides (Malamud et al., 2004). The difficulty resides in acquiring information on surface and sub-surface geometry for a large number of landslides, and can only be solved, at present, adopting empirical relations that link geometrical measurements, such as the individual landslide area, with its volume. Several authors have suggested that there is a relationship between the area and the volume of landslides that can be expressed through empirical formulations (Simonett, 1967; Rice and Fogging, 1971; Innes, 1983; Guthrie and Evans, 2004; Korup, 2005; ten Brink et al., 2006; Imaizumi and Sidle, 2007; Guzzetti et al., 2008; Imaizumi et al.. 2008). Furthermore, Guzzetti et al. (2009) state that the relationship is largely geometrical and not significantly influenced by mechanical or geomorphological properties.

3 Regional setting

Madeira is a within-plate North Atlantic volcanic island located approximately 600 km northwest of the western African coast (Fig. 1). The island is the exposed part of a massive stratovolcano about 6 km high, resting on a 130 Ma old oceanic crust (Schminke, 1982). The island, almost completely formed by volcanic materials, has an approximately E–W-elongated form (58 km long and 23 km wide) with the topographic axis running in the same direction and a total surface area of 737 km^2. Madeira is renowned for its spectacular landscapes, with impressive "V"-shaped valleys, very steep slopes and rugged sea-cliffs; 90 % of its surface is above 500 m in altitude and 35 % is above 1000 m, with a maximum altitude of 1862 m at Pico Ruivo (Carvalho and Brandão, 1991). The orography influences local climate: the main mountain axis is perpendicular to the direction of the predominant winds, which results in different temperature and precipitation rates in different parts of the island (Prada and Serralheiro, 2000). The main erosion agent is precipitation, which strongly affects the hydrographic network and the wave climate, which works in the coastal zones (Carvalho and Brandão, 1991). The stream system does not carry a regular flow of water and their regimen can be considered torrential. The main areas affected by the 2010 event belong to the municipalities of Ribeira Brava and Funchal (Fig. 2) both in the southern slopes but non-adjacent. Ribeira Brava municipality includes two main drainage basins: Tabua and Ribeira Brava, with areas of 8.8 km^2 and 40.9 km^2, respectively, for a total of 49.7 km^2. The Funchal area includes three main drainage basins: São João (14.7 km^2), Santa Luzia (15.6 km^2) and João Gomes (11.4 km^2), for a total area of 41.7 km^2.

According to Prada and Serralheiro (2000), the basins of São João, Santa Luzia, João Gomes and Tabua present a parallel drainage pattern, typical of recent volcanic formations, with elongated shape. The transverse profiles of the valleys are very deep and "V"-shaped and the drainage channels are parallel to sub-parallel among them and exoreic. The Ribeira Brava basin is funnel shaped in planar view, with a dendritic drainage upstream pattern and a paralleled composed dendritic downstream pattern, both exoreic.

4 Characterisation of the landsliding event

On 20 February 2010, the regions of Funchal and Ribeira Brava have suffered intense and diffused landsliding. Field surveys by the local Forestry Services allowed the in situ identification of 233 landslides, classified as both soil slips and soil slips debris flows (Fig. 2). Soil slips are characterised by small size and thickness (up to 1.5 m), with volumes up to few cubic metres. Furthermore, these shallow landslides were, in some cases, the primary source of larger slides, developing into debris flows. Failing mass advances as a debris flow, completely evacuating the scar, and flows down to the valley bottom, dragging material along the way. The morphology of the debris flows is confined laterally where natural channels are present (Fig. 2d); otherwise they progressively increase in width along the slopes (Fig. 2c and e). As

a consequence, small initial slides (Fig. 2c and d) can affect wide portions of the slopes. In rare cases they are associated with the reactivation of older soil slip-debris flows scars.

5 Base information

The base information available for the inventory and mapping of the mass movements includes the following datasets:

- Multispectral GeoEye-1 satellite images (R-G-B-NIR bands with spatial resolution of 2 m pixel^{-1} and PAN band with 0.5 m pixel^{-1}) acquired in pre-event (21 and 29 July 2009) and post-event dates (23 and 28 February 2010).
- Orthophotomaps, provided by the regional territorial management agency (DRIGOT), with pre-event (2007) and post-event (2010) dates, with RGB bands with 0.4 m pixel^{-1} of spatial resolution.
- digital elevation models (DEMs) provided by DRIGOT, with pre- and post-event dates and in regular grid format:
  - Pre-event DEM (2007), obtained by aerophotogrammetry, 1 : 5000 scale and 10 m final resolution, precision 1 m.
  - Pre-event DEM (2009), obtained by LIDAR surveying, 1 : 2000 scale and 4 m of final resolution.
  - Post-event DEM (2010), obtained by aerophotogrammetry, 1 : 5000 scale and 10 m final resolution, precision 1 m.
- The 2009 edition of the Madeira Geological Map (1 : 80 000 scale) provided by the Portuguese Laboratory of Engineering and Geology (LNEG), in shape-file format.
- The 2007 edition of the Madeira Land Cover Map (1 : 10 000 scale), and 5 hierarchical levels of classification (compatible with the CORINE Land Cover classification).
- Miscellaneous field survey data, pre and post event, provided by several sources (agencies, companies and the local university). This includes:
  - Field identification of landslides of the 20 February event (maps, field forms).
  - GNSS-based surveys resulting on maps of the landslide shapes, limits and height.
  - Topographic surveys of several landslide scars surfaces.
  - Landslide photographs (ground-based).

6 Satellite image processing

6.1 Pre-processing

In order to integrate and use all the available information, a pre-processing stage had to be applied to all the GeoEye-1 satellite images available, guaranteeing data standardisation. The images already had radiometric correction, so the pre-processing stage focused on the geometric correction. Because Madeira Island is an area with very steep slopes, the previous rectification made by the image supplier (without 3-D terrain information) was manifestly insufficient. The raw images had strong geometric distortions which prevented the correct alignment between them, and thus geometric correction was essential. The tasks developed in this stage consisted mainly in (i) co-registration, (ii) band-fusion, and (iii) orthorectification. The software ENVI 4.7 (Exelies Visual Information Solutions) was used for the image pre-processing and processing stages.

For the pansharpening action to be effective, band images of interest had to be closely aligned. The native georeferencing information that is delivered with the imagery is typically not accurate enough for this purpose, and a co-registration process was necessary. This was completed selecting tie points marking the same features on both band images, allowing the correct co-registration between different bands. The co-registration process used 30 to 60 tie points, minimizing root mean square (RMS) errors. The warp method was the polynomial and the nearest neighbour method was chosen as the warp interpolation algorithm. Next, a layer stacking between the bands R-G-B-NIR, and between the last one and the PAN band, was necessary. This allowed the resampling and re-projection to a common user-selected output projection (UTM – zone 28° N, Datum WGS-84) maintaining the pixel size of 2.0 m. The resampling method used was the nearest neighbour.

The band-fusion process, namely the pansharpening method, is a technique in which high-resolution panchromatic data is merged with lower resolution multispectral data to create a colorized high-resolution dataset. In this specific case, we obtained the high ground sampling resolution (0.5 m provided by the PAN band). The pansharpening fusion method used was the Gram-Schmidt method available in ENVI software.

The last step in the pre-processing stage was the orthorectification of the final pansharpened images. These steps required the use of a DEM and, in order to collect the respective DEM points, the use of orthophotomaps was also necessary. Because two DEMs with different resolutions were available for the orthorectification process, a previewing evaluation of the errors associated with the use of each DEM was conducted. The mean RMSE (root mean square or quadratic mean deviation) were 2.15 m for the 2007 DEM and 1.34 m for the 2009 DEM. For each satellite image, two sets of control points were selected: one for the multispectral stack

R-G-B-NIR and a second one for the pansharpened image, both connected to the 2009 DEM. For each set of control points the list was reviewed, and the points with the highest values of RMSE were deleted. This method also makes use of the RCP (Rationale Polynomial Coefficients), which provides a compact representation of the ground-to-image geometry.

6.2 Classification

6.2.1 Supervised automatic classification

The pixel based classification method, intended to identify landslide scars, was conducted on both post-event GeoEye-1 images (23 and 28 February 2010) to assure the total coverage of the affected area. Several supervised classification methods were tested, but preliminary results showed that the maximum likelihood supervised method (where pixels are assigned to the class of highest probability) achieved the best results, with an overall accuracy of 93.6 % for a separate ground-truth set, besides being an easy and computationally efficient method (Table 1). This method, based on the statistical descriptors of each selected class, allowed the semi-automatic classification of each pixel of the multispectral image. The construction of the training dataset was made using the ancillary data and to some extent with field knowledge.

The pixel based classification procedure intends to target the landslide scars. These scars not always exhibit a regular contour, or the initial and deposition points are not always clear. Soil slips usually exhibit more regular contours, but soil slip-debris flow occurrences are more complex. Nevertheless, even the soil slips had features that could bias the classification, such as the landslide track (vegetation that has been brushed at the passage of the sliding material, but with no scour or deposition), or deposition/scour areas. A total of 12 classes were defined: (1) recent landslide scar, (2) landslide track (principal path of the slipped material), (3) non-recent landslide scar, (4) bare soil, (5) undergrowth vegetation, (6) trees/Forest (general), (7) gravel or accumulation of coarse material, (8) roads (general), (9) large infrastructure elements (warehouses, factories), (10) house roofs, (11) shaded areas, and (12) cloud covered areas. Both the Funchal and Ribeira Brava regions were classified with the same number of classes, but the training stage was conducted separately, in order to maximise the accuracy of the classification method and eliminate potential environmental differences (solar illumination, atmospheric conditions and relief shadows).

6.2.2 Post-processing

Although the classification method had a good overall result, some typical classification errors of a pixel-based classification were perceived. As such, the next stage consisted in filtering and reclassifying the isolated and small groups of pixels. The filtering stage enabled an overall classification improvement through the analysis of the classified map in terms of the neighbourhood of each classified pixel, i.e. it was assumed that a group of pixels (5×5 pixels) of a certain class that is surrounded by a majority of pixels belonging to another class does not have expression – therefore it should be filtered and the pixels should be assigned to the majority class. Sieving and clump methods (Canty, 2010) were used. The robustness of these filters assured a clear improvement of the spatial structure of the classified map (Fig. 3). Raster classified maps were converted to vector layers, where each scar is defined by a polygon, necessary for the validation stage.

Table 1. Overall accuracy and kappa coefficient* for the ground truth set associated with each supervised method tested.

Supervised methods	Overall accuracy (%)	Kappa coefficient
Maximum likelihood	93.6	0.92
Minimum distance	80.4	0.74
Mahalanobis distance	81.0	0.75

* The kappa coefficient is a quantification measuring the degree of agreement of a classification.

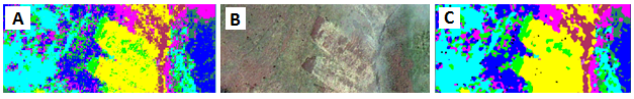

Fig. 3. Filtering operation: detail of improvement on the spatial structure of the classified map. **A** – classified map; **B** – GeoEye-1 satellite image, and **C** – filtering operation result. Scars are represented in green, landslide tracks in yellow, vegetation in dark blue, bare soil in bright blue, clouds in pink and gravel in bordeux. Note the perfect differentiation between landslide track and bare soil, which, a priori, would be the most similar classes.

6.2.3 Validation stage

After the classification stage, an expert validation of the results was conducted. The process consisted of a visual inspection and a comparison of all the final classified polygons with the satellite and orthophotomap imagery, both pre- and post-event, editing the polygon outlines that presented poor results or adding new ones. This ensures that the identified polygons belonged only to recent landslide scars, or to those recently activated (Fig. 4). This task was particularly important because the images had large regions with dense atmospheric coverage (clouds) and poorly illuminated (shaded) areas due to the steep orography (Fig. 5). The Ribeira Brava satellite images had 20 % of their area occupied by either clouds or shaded areas, whereas the Funchal area only had 2 %. The use of the ortophotomaps, with less shaded areas, allowed a significant improvement of the initial classification, with the delineation of several landslides that could not be recognized on the satellite imagery.

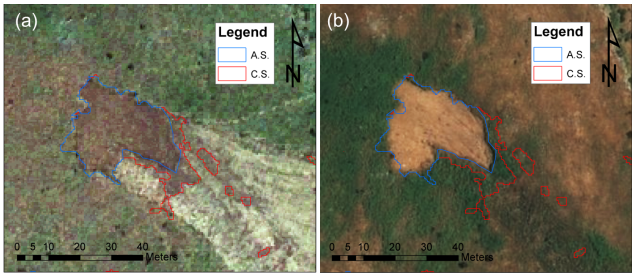

Fig. 4. Example of an edited polygon: in blue the edited contour (A.S.) and in red the contour extracted during the classification procedure (C.S.). **(a)** GeoEye1 image and **(b)** the orthophotomap.

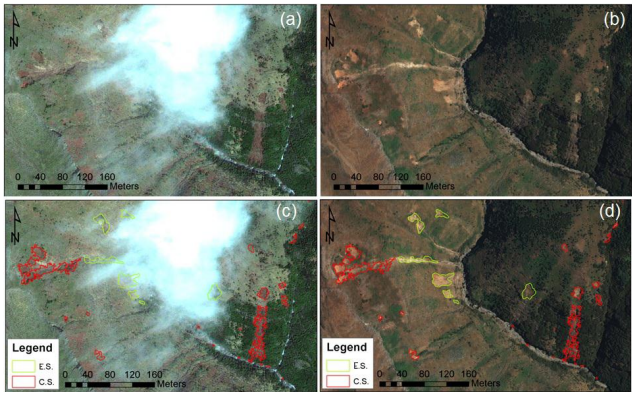

Fig. 5. Example of added polygons: in red the contours extracted during the classification procedure (C.S.) and in green the contours added because of clouds and shadows (L.S.). On the left GeoEye imagery, and on the right orthophotomaps used for correct the classification.

In this final step, Classes 1 and 3 of the classification stage were reclassified in 3 new classes:

- Class 1 – recent landslide scars, with well-defined edges and apparent depth, not identified on the pre-event orthophotomaps or satellite images.
- Class 2 – old landslide scars, on pre-event images.
- Class 3 – recent landslide scars, with ill-defined perimeter and not exhibiting an apparent depth.

A total of 8465 polygons were identified for the three classes: 5174 in the Ribeira Brava area and 3291 in the Funchal area, representing only 1.6 % of the classified total. This discrepancy can be explained not only because Ribeira Brava had a larger clouded/shadowed area, but also because the region has a steeper terrain and the images were taken right after the event, when a lot of mud trail was still present, thus turning the girth of the polygons larger.

This step culminated in a complete inventory of the pre- and post-event landslides, which can be observed in Figs. 6 and 7. The percentages of landslide scars that were correctly classified was calculated using a ground truth set of geographical locations for 233 landslide scars identified in the

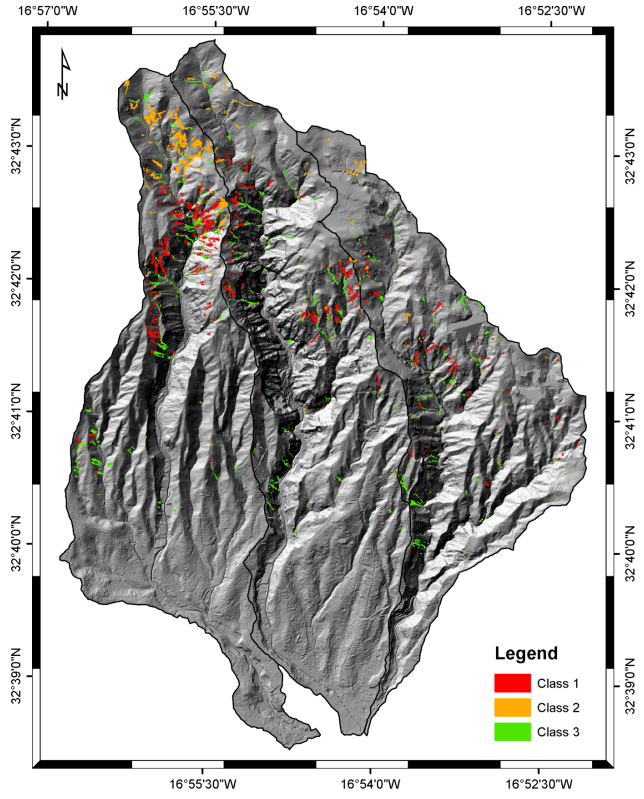

Fig. 6. Landslide inventory map for the Funchal area.

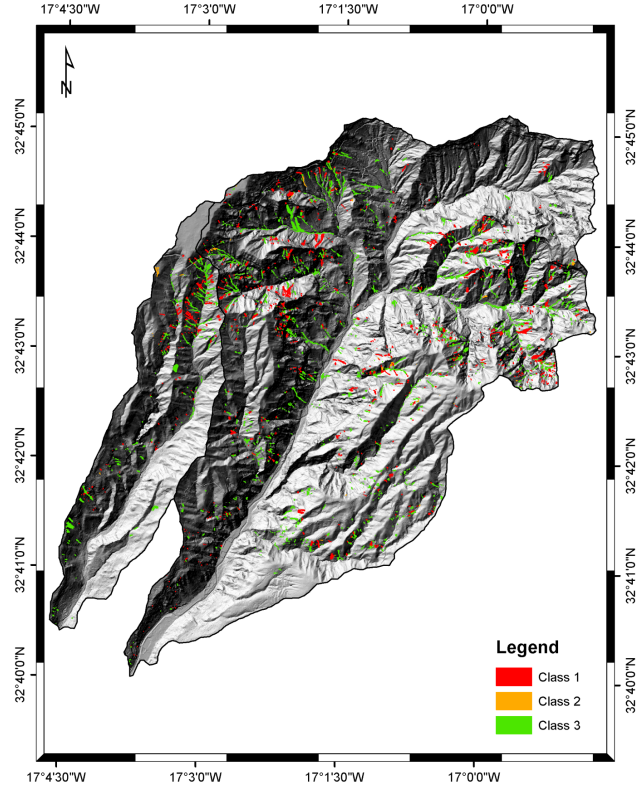

Fig. 7. Landslide inventory map for the Ribeira Brava area.

Table 2. Overall results of the validation stage. LC – number of landslide polygons classified; LI – number of landslides identified in the field; LCC – Landslide polygons correctly classified; and LNI – Landslides not identified in the images.

Basins	LC	LI		LCC		LNI	
		#	%	#	%	#	%
João Gomes	708	21	3.0	20	95.2	1	4.8
Santa Luzia	1039	29	2.8	28	96.6	1	3.4
São João	1544	73	4.7	70	95.9	3	4.1
Ribeira Brava	4583	95	2.1	76	80.0	19	20.0
Tabua	591	15	2.5	13	86.7	2	13.3

field by the Madeira Island Forestry Services with a good spatial coverage, representing the landslide population in our study area. The overall results of the validation stage (Table 2) suggest that the classification results are very good, showing a high success rate in the landslide scar identification: 96 % of the landslides were identified in Funchal and 83 % in Ribeira Brava.

In what regards the contribution of the orthophotomaps for identification of the landslides, the situation was different for the Funchal and Ribeira Brava basins, due to their different relief conditions. In Ribeira Brava, where shadow areas were larger in the VHR satellite images, 1003 landslides have been included after the orthophotomap examination, whereas in Funchal basin, this figure was much smaller (138). For the entire study area, the overall performance of the semi-automatic procedure was such that about 13 % of the landslides were identified due to the orthophotomap ancillary data and about 87 % were identified by the classifier on the GeoEye images.

7 Landslide sediment volume estimation

After the completion of the landslide scars inventory, it was possible to estimate the amount of sediment produced in this event. Part of this sediment fed the flash flood by becoming entrained in the hydrographical network clinging, while the other part is still available upstream, waiting for future heavy rain events to be displaced. The first attempt to calculate the displaced sediment volume was made using the two available pre- and post-event DEMs. However, the resolution of the most recent DEM was not adequate to account for the small size of the landslides. The 2010 DEM presented a maximum resolution of 10 m, a value that was very similar to the length of several landslides, thus making the delineation of the landslides impossible. Instead of the DEM difference, a more straightforward approach was tested as described below.

We followed the procedure proposed by Guzzetti et al. (2009), in which a volume-area scaling empirical relationship with the form:

Table 3. Minimum and maximum landslide volumes for the two affected areas: Class 1: new scars; Class 2: old scars (prior to the 20 February event); and Class 3: new scars, but shallow and poorly identified.

Study area	Classes	Area (m^2)	Volume 30 landslides	Volume according to Guzzetti (2009)
Ribeira Brava	1	292.236	278.932	477.497
	2	10.345	7.816	10.106
	3	385.009	326.058	506.875
Funchal	1	151.661	147.387	257.417
	2	108.300	129.379	283.768
	3	100.946	69.473	86.583

$$V_L = \alpha A_L^{\gamma}, \quad (1)$$

was obtained using a global catalogue of landslides, with the scaling parameters as follows:

$$\alpha = 0.074 \quad \text{and} \quad \gamma = 1.450,$$

where α and γ are power-law scaling parameters.

The best-fit line for the data measured on the field from our 30-landslide set (see details in Sect. 7.1.1) resulted in the following relationship:

$$V_{30} = 0.22 A_L^{1.22} \quad (2)$$

which is in agreement with the relationship obtained by Guzzetti et al. (2009) as shown later in Fig. 10.

The sediment volume estimations were calculated using both scaling relationships, bracketing in this way the range of variation. The volume is estimated based only on the landslide scar area.

The minimum value was obtained using Eq. (2). For this case, the calculated sediment volume produced from the 2010 event, landslides, using Classes 1 and 3, was ca. 217 000 m^3 for Funchal basins (total). In the case of the Ribeira Brava basins a total of 605 000 m^3 was estimated (Table 3).

For the Funchal area, percentages of area covered by the landslide scars were determined separately for the three main sub-basins. The highest percentage of affected area is 0.29 %, 0.19 % and 0.12 %, which translates into a higher volume produced in São João basin, followed by Santa Luzia and João Gomes basins, respectively. In the case of Ribeira Brava study area, results show that the difference between the two main basins is even greater. The Ribeira Brava basin has 1.37 % of affected area, while Tabua only has 0.25 %. These results translate into a much higher volume of mobilized material in the Ribeira Brava basin when compared with any other of the considered basins, having a volume almost five times larger than the remaining basins (Fig. 9).

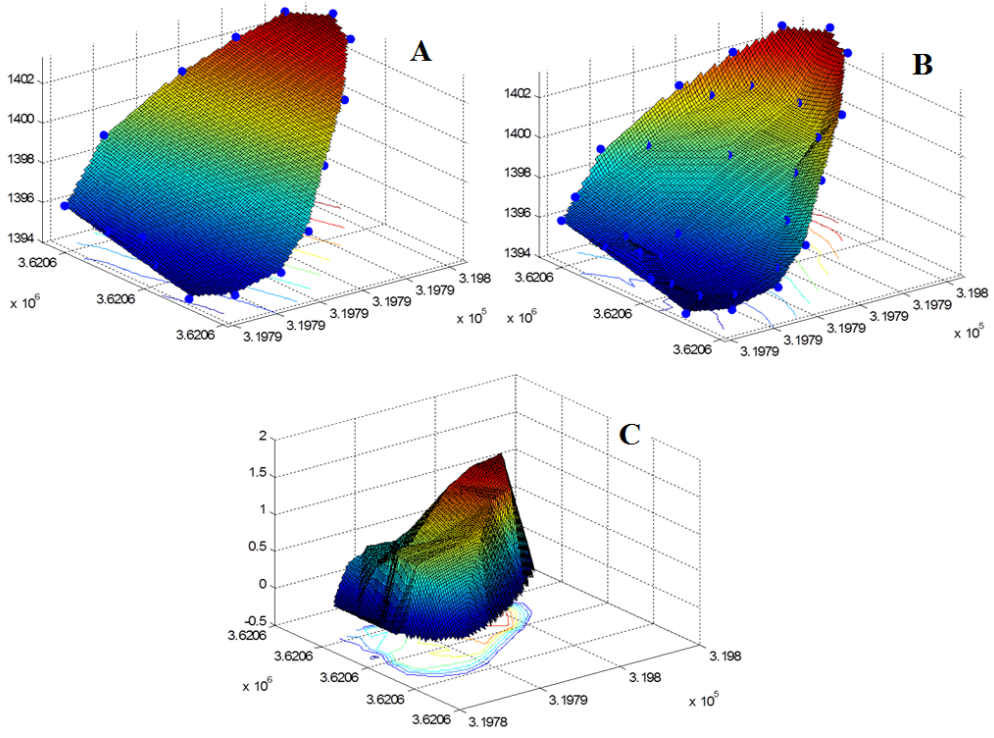

Fig. 8. Example of the modelling of the landslides surveyed in the field: **A** – original reference surface; **B** – landslide scar surface and **C** – model of the landslide slide material.

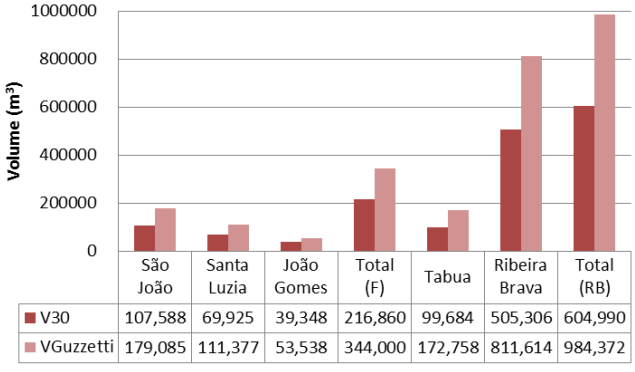

	São João	Santa Luzia	João Gomes	Total (F)	Tabua	Ribeira Brava	Total (RB)
V30	107,588	69,925	39,348	216,860	99,684	505,306	604,990
VGuzzetti	179,085	111,377	53,538	344,000	172,758	811,614	984,372

Fig. 9. Estimated volume for each affected basin and for each considered equation. F – Funchal municipality and RB – Ribeira Brava municipality.

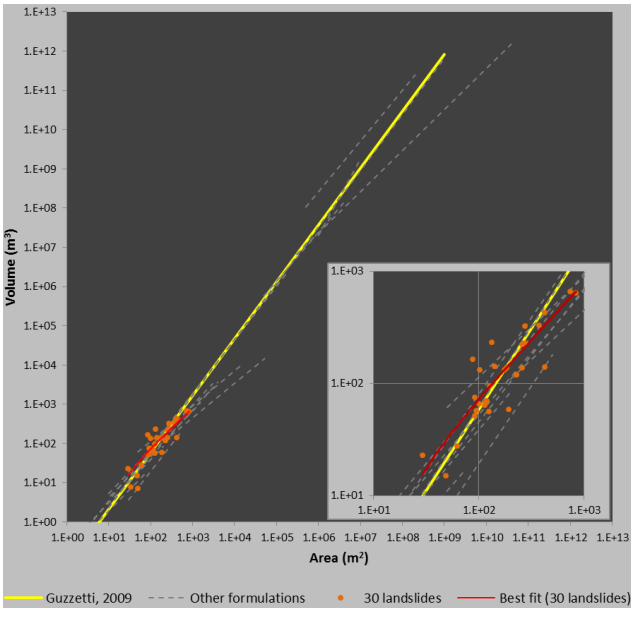

Fig. 10. Area versus Volume (V_L) projection for the empirical formulations. Detail of the Madeira landslides area and volume ranges (right bottom). Other formulations relates to all the formulation used in Guzzetti (2009).

7.1 Validation

7.1.1 Field data

A total of 30 landslide scars, scattered around the study area and representative of the soil-slips population, was surveyed in situ using GNSS devices (relative positioning), and total station and depth measurements were registered. From the surveyed landslides it was possible to obtain two different surfaces: one referring to the original reference surface and another to the landslide scar surface. The difference between

both surfaces gives us the amount of material removed, allowing the modelling of the surface of the slide material (Fig. 8). The complete methodology is described in Lira et al. (2011b). This model allowed calculating the dislocated volume of each landslide, and the calculations of the depth statistics of landslide scars (average of 0.86 m for the Ribeira Brava area and 0.60 m for the Funchal area, maximum depths of 1.87 m for the Ribeira Brava and 1.18 m for Funchal).

7.1.2 Area/volume empirical formulation

In order to test the applicability of the volume assessment, the following aspects were considered: (a) the area and volume of the 30 landslides surveyed in the field, (b) the empirical formulation presented by Guzzetti et al. (2009), and (c) the best fit for the 30 surveyed landslides (Eq. 2). The results can be seen in Fig. 10.

Equation (2) projection line (red line) exhibits a different slope value from the Guzzetti et al. (2009) formulation (yellow line). This means that Eq. (2) will produce volume values smaller than the Guzzetti formulation for area values greater than 10^2 m^2, and volume values greater for areas smaller than 10^2 m^2. The projection of the 30 landslides seems to suggest that the formulation of Guzzetti et al. (2009) slightly overestimates the volumes for the range of A_L (10^1–10^3 m^2) in the study region. Additionally, Eq. (2) exhibits the same slope angle that other empirical formulations which consider the same type of landslides and A_L ranges, while the Guzzetti formulation considers all type of landslides, for all ranges of A_L (ranging from 10^1 to 10^{10} m^2). The root mean square error (RMSE) for the Guzzetti formulation is 157, while the RMSE for Eq. (2) is only 63, which means that the Guzzetti formulation is overestimating (doubles) landslide volume.

8 Discussion

A significant part of the coarser sediment material transported by the Funchal stream network during the studied event was deposited in the lower part of the network and on the streets of Funchal city – as there were episodes of massive overtopping of river banks by the flash flood, while the fine-grained fraction was washed out to the sea. The regional administration estimated the volume of the landfill deposited by the Funchal wharf as a consequence of the cleaning work of Funchal streets and the lower section of the stream channels on 140 000 m^3. In addition to this volume, the dredged material from the port area, ca. 100 000 m^3, should also be considered. Taking into account all the above volume estimations, it is estimated that for the Funchal area alone, at least 250 000 m^3 of sediment material was deposited downstream.

The estimated landslide volumes for each area and class can be observed on Table 3. Landslides were concentrated mainly upstream in both areas (Figs. 6 and 7).

The percentage of the total area affected by landslides was 0.61 % for the Funchal basins and 1.36 % for Ribeira Brava basins. As such, the proportion of affected area in Ribeira Brava was roughly the double that of the affected area in Funchal. In terms of the corresponding volumes, as the Ribeira Brava affected area is almost three times larger than the Funchal case, the Ribeira Brava basins were also affected more during the event than the Funchal basins when compared with the total area occupied by each basin. From this study it is also possible to estimate the volume of past landslide events, as these were identified and classified (Class 2). The affected area for Class 2 in the Funchal area was 0.26 % and in Ribeira Brava basins only 0.02 %. This seems to suggest that the studied event was an extremely damaging one in Ribeira Brava and that a similar episode did not occur in a recent past. The Funchal area seems to be especially susceptible to this type of events, since the percentage of recent past landslides is high, when compared with the same ratio for Ribeira Brava.

Unfortunately, data is only available for the quantity of the sediment that reached the downstream regions of the Funchal basins, disabling a comparison with the landslide estimated volumes on other areas. The triggering landslide event and the flash flood occurred almost simultaneously, which resulted in the feeding of the flood itself with landslide material. Nevertheless, some sediment always accumulates along the landslide paths. It is thus expectable that the sediment volume estimated from the displaced volume of landslide material will be different from that volume estimated from material deposited in the downstream regions. It is only possible to compare the landslide volume values with the landfill and fine-grained sedimentary material values (250 000 m^3). For the sedimentary budget the value of ca. 217 000 m^3, the amount of volume is not enough to account for all the sediment volume reaching the downstream regions. This result seems to translate that there was a large amount of sediment material accumulated on river beds that was eroded and transported downstream during this particular flash flood, and that the landslides which occurred did not account for all the material reaching the downstream regions. Additionally, the expert validation stage also was able to identify that there are recent sediment deposits created during this event ready to be mobilized by future rainfalls.

9 Conclusions

The extent of the affected area and the number of landslides triggered during the 2010 event in Madeira Island called for the use of a semi-automated processing and analytical methodology for the rapid landslide identification. The type of landslides that occurred in the studied event (numerous, mostly small, disperse and shallow) and the hazardous and inaccessible terrain characteristics of the most part of affected areas, thus invalidating extensive field work,

made the use of high resolution multispectral satellite images a necessity. The established methodological approach was a simple and computationally efficient approach to identify the landslide scars. Nevertheless, an expert validation stage was still necessary, because the spectral characteristics of the landslide scars did not allow the subdivision into distinct classes. The final step consisted in the production of a landslide inventory map for each study area. The affected area by landslides was about 0.61 % in Funchal basins and 1.36 % in Ribeira Brava basins. The inventory maps also allowed estimating the mobilized volume using empirical scaling relationships based on local and global field data. The estimated displaced volume ranges from 217 000 m^3 to 344 000 m^3, and 605 000 m^3 to 984 000 m^3 for Funchal and Ribeira Brava basins, respectively. Quantifying the displaced landslide volumes and mapping the sources helped in the design and implementation of measures to prevent damages caused by landslides in Madeira Island.

Future work will involve the use of the landslide inventory maps with additional terrain information, in order to better understand the triggering factors for this specific region and the variables that may affect and facilitate failure.

Acknowledgements. The authors would like to thank the geology teams of the University of Madeira (UMA) and of the Instituto Superior Técnico (IST) and the topographic team of the Direcção Regional de Informação Geográfica e Ordenamento do Território (DRIGOT), for providing the field work, and the DRIGOT direction for the satellite images and geographical information data. This study was developed in the framework of the projects: "Evaluation of the risk of alluvium in Madeira Island – EARAM" funded by the Secretaria Regional de Equipamento Social of Madeira and "AULIS" – Automated landslides inventory based on very high spatial resolution images (PTDC/ECM/116611/2010) funded by Fundação para a Ciência e Tecnologia (FCT).

Edited by: M.-C. Llasat
Reviewed by: O. Petrucci and J. Corominas

References

Aleotti, P.: A warning system for rainfall-induced shallow failures, Eng. Geol., 73, 247–265, 2004.

Almeida, A., Oliveira, R. P., França, P., Rodrigues, D., Silva, D. F., Lopes, S. S., Magro, C., Lopes, A., Fragoso, M., Alcoforado, M. J., Portela, M., Saint-Maurice, G., Silva, A., Cardoso, A. H., Ferreira, R., Queirós, G. T., Coutinho, M. A., Sousa, A. J., Heleno, S., Gonçalves, A., Paula Falcão, A. P., Pereira, M. J., Pina, P., Lira, C., Matias, M., Lousada, M., Santos, J. A., Lopes, I., Pereira, M. F., Dionísio, A., Abreu, U., Cardoso, R., Vieira, F., Sequeira, M., Jesus, J., Correia, A. P., Figueiredo, A., Azevedo, J., Prada, S., Reis, J. A., Spínola, A. V., Figueira, C., Aguiar, N., Teixeira, H., Castro, J., Fernandes, D., and Neves, M. J.: Estudo de avaliação de risco de aluviões na ilha da Madeira, Final Report, Instituto Superior Técnico, Lisboa, 1008 pp., 2010 (in Portuguese).

Ardizzone, F., Cardinali, M., Galli, M., Guzzetti, F., and Reichenbach, P.: Identification and mapping of recent rainfall-induced landslides using elevation data collected by airborne Lidar, Nat. Hazards Earth Syst. Sci., 7, 637–650, doi:10.5194/nhess-7-637-2007, 2007.

Bucknam, R. C., Coe, J. A., Chavarria, M. M., Godt, J. W., Tarr, A. C., Bradley, L. A., Rafferty, S., Hancock, D., Dart, R. L., and Johnson, M. L.: Landslides Triggered by Hurricane Mitch in Guatemala – Inventory and Discussion, U.S. Geological Survey, Open File Report 01–443, 2001

Canty, M. J.: Image Analysis, Classification and Change Detection in Remote Sensing: With algorithms for ENVI/IDL, 2nd Edn., CRC Press, 441 pp., 2010.

Cardinali, M., Ardizzone, F., Galli, M., Guzzetti, F., and Reichenbach, P.: Landslides triggered by rapid snow melting: the December 1996–January 1997 event in Central Italy, in: Proceedings of the 1st EGS Plinius Conference, edited by: Claps, P. and Siccardi, F., Bios Publisher, Cosenza, 2001.

Carvalho, A. M. G. and Brandão, J. M.: Geologia do Arquipélago da Madeira, Museu de História Natural, Lisboa, Portugal, 170 pp., 1991 (in Portuguese).

Corsini, A., Borgatti, L., Coren, F., and Vellico, M.: Use of multitemporal airborne LiDAR surveys to analyse post-failure behaviour of earthslides, Can. J. Remote Sens., 33, 116–120, 2007.

Cruden, D. M. and Varnes, D. J.: Landslide types and processes, in: Landslides: Investigation and Mitigation, edited by: Turner, A. K. and Shuster, R. L., Transportation research board, Special report, 247, 36–75, 1996.

Danneels, G., Pirard, E., and Havenith, H. B.: Automatic landslide detection from remote sensing images using supervised classification methods. Proceedings of IGARSS2007, IEEE International Geoscience and Remote Sensing Symposium, 3014–3017, 2007.

Dong, J. J., Lee, C. T., Tung, Y. H., Liu, C. N., Lin, K. P., and Lee, J. F.: The role of the sediment budget in understanding debris flow susceptibility. Earth Surf. Proc. Land., 34, 1612–1624, 2009.

Fernández, T., Jiménez, J., Fernández, P., El Hamdouni, R., Cardenal, F. J., Delgado, J., Irigaray, C., and Chacón, J.: Automatic Detection of Landslides features with remote sensing techniques in the Betic Cordilleras (Granada, Southern Spain), The International Archives of Photogrammetry, Remote Sensing and Spatial Information Science, XXXVII (Part B8), 351–356, 2005.

Fragoso, M., Trigo, R. M., Pinto, J. G., Lopes, S., Lopes, A., Ulbrich, S., and Magro, C.: The 20 February 2010 Madeira flash-floods: synoptic analysis and extreme rainfall assessment, Nat. Hazards Earth Syst. Sci., 12, 715–730, doi:10.5194/nhess-12-715-2012, 2012.

Galiatsatos, N., Donoghue, D. N. M., and Warburton, L.: Assessment of sediment delivery from shallow landslides in upland terrain using 3D remote sensing, in: RSPSoc2007: Challenges for earth observation – scientific, technical and commercial, Newcastle, UK, 2007

Giannecchini, R.: Relationship between rainfall and shallow landslides in the southern Apuan Alps (Italy), Nat. Hazards Earth Syst. Sci., 6, 357–364, doi:10.5194/nhess-6-357-2006, 2006.

Guthrie, R. H. and Evans, S. G.: Analysis of landslide frequencies and characteristics in a natural system, coastal British Columbia, Earth Surf. Proc. Land., 29, 1321–1339, 2004.

Guzzetti, F., Cardinali, M., Reichenbach, P., Cipolla, F., Sebastiani, C., Galli, M., and Salvati, P.: Landslides triggered by the 23 November 2000 rainfall event in the Imperia Province, Western Liguria, Italy, Eng. Geol., 73, 229–245, 2004.

Guzzetti, F., Ardizzone, F., Cardinali, M., Galli, M., Reichenbach, P., and Rossi, M.: Distribution of landslides in the Upper Tiber River basin, central Italy, Geomorphology, 96, 105–122, 2008.

Guzzetti, F. Ardizzone, F., Cardinali, M., Rossi, M., and Valigi, D.: Landslide volumes and landslide mobilization rates in Umbria, central Italy, Earth Planet. Sc. Lett., 279, 222–229, 2009.

Imaizumi, F. and Sidle, R. C.: Linkage of sediment supply and transport processes in Miyagawa Dam catchment, Japan, J. Geophys. Res., 112, F03012, doi:10.1029/2006JF000495, 2007.

Imaizumi, F., Sidle, R. C., and Kamei, R.: Effects of forest harvesting on the occurrence of landslides and debris flows in steep terrain of central Japan, Earth Surf. Proc. Land., 33, 827–840, 2008.

Innes, J. N.: Lichenometric dating of debris-flowdeposits in the Scottish Highlands, Earth Surf. Proc. Land., 8, 579–588, 1983.

Kasai, M., Ikeda, M., Asahina, T., and Fujisawa, K.: LiDAR-derived DEM evaluation of deep-seated landslides in a steep and rocky region of Japan, Geomorphology, 113, 57–69, 2009.

Kirschbaum, D. B., Adler, R., Hong, Y., Hill, S., and Lerner-Lam, A.: A global landslide catalog for hazard applications: method, results, and limitations, Nat. Hazards, 52, 561–575, 2009.

Korup, O.: Distribution of landslides in southwest New Zealand, Landslides, 2, 43–51, 2005.

Lira, C., Lousada, M., Falcão, A. P., Gonçalves, A., Heleno, S., Matias, M., de Sousa, A. J., Pereira, M. J., Pina, P., Oliveira, R., and Almeida, A. B.: Automatic Detection of Landslide features with remote sensing techniques: Application to Madeira Island, in: Proceedings of IGARSS 2011 – IEEE Geoscience and Remote Sensing Symposium, 1997–2000, Vancouver, Canada, 2011a.

Lira, C., Falcão, A. P., Gonçalves, A., Heleno, S., Lousada, M., Matias, M., Sousa, A. J., Pereira, M. J., Pina, P., Oliveira, R., and Betâmio de Almeida, A.: Landslide shape modeling from field cartography, EGU General Assembly, Vienna, Austria, 3–8 April 2011, 13, EGU2011-11324-1, 2011b.

Liu, J.-K., Chang, K.-T., Rau, J.-Y., Hsu, W.-Ch., Liao, Z.-Y., Lau, Ch.-Ch., and Shih, T.-Y.: The Geomorphometry of Rainfall-Induced Landslides in Taiwan Obtained by Airborne Lidar and Digital Photography, edited by: Ho, P.-G. P., Geoscience and Remote Sensing, 598 pp., doi:10.5772/8305, 2009.

Malamud, B. D., Turcotte, D. L., Guzzetti, F., and Reichenbach, P.: Landslide inventories and their statistical properties, Earth Surf. Proc. Land., 29, 687–711, 2004.

Martha, T. R., Kerleb, N., Jettenb, V., Van Westenb, C. J., and Kumara, K. V.: Characterising spectral, spatial and morphometric properties of landslides for semi-automatic detection using object-oriented methods, Geomorphology, 116, 24–36, 2010.

McKeana, J. and Roering, J.: Objective landslide detection and surface morphology mapping using high-resolution airborne laser altimetry, Geomorphology, 57, 331–351, 2004.

Nichol, J. and Wong, M. S.: Detection and interpretation of landslides using satellite images, Land Degrad. Dev., 16, 243–255, 2005.

Prada, S. and Serralheiro, A.: Stratigraphy and evolutionary model of Madeira Island, Museu Municipal Funchal, Bocagiana 200, 13 pp., 2000.

Rice, R. M. and Foggin, G. T.: Effects of high intensity storms on soil slippage on mountainous watersheds in Southern California. Water Resour. Res., 7, 1485–1496, 1971.

Rodrigues, D. and Ayala-Carcedo, F. J.: Georisks a natural hazard database of historic events in Madeira Island, 25th General Assembly E.G.S., Nice, 286 pp., 2000.

Rodrigues, D. and Ayala-Carcedo, F. J.: Rain induced landslides and debris flows in Madeira Island Portugal, Landslide News, Landslide News, 14/15, 43-45, 2003a.

Rodrigues, D. and Ayala-Carcedo, F. J.: Slides in Madeira island, ISRM International Symposium on RockEngineering for Moutainous Regions, Funchal, 223–230, 2003b.

Schminke, H. U.: Volcanic and chemical evolution of the Canary Islands, in: Geology of the Northwest African continental margin, edited by: von Rad, U., Hinz, K., Sarnthein, M., and Seibold, E., Springer-Verlag, Heidelberg, Germany, 273–305, 1982.

Schulz, W. H.: Landslide susceptibility revealed by LIDAR imagery and historical records, Seattle, Washington, Eng. Geol., 89, 67–87, 2007.

Simonett, D. S.: Landslide distribution and earthquakes in the Bewani and Torricelli Mountains, New Guinea, in: Landform Studies from Australia and NewGuinea, edited by: Jennings, J. N. and Mabbutt, J. A., Cambridge University Press, Cambridge, 64–84, 1967.

SRA/INAG: Plano Regional de Água da Madeira, Secretaria Regional do Ambiente/Instituto da Água, Funchal, 2003 (in Portuguese).

Takara, K., Yamashiki, Y., and Ibrahim, A. B.: Assessment of Spatially-Distributed Sediment Budget and Potential Shallow Landslide Area for Investment Prioritization in Sediment Control of Ungauged Catchment: A Case Study on the upper Citarum River, Indonesia, Disaster Prevention Research Institute Annuals B, 53, 45–60, 2010.

ten Brink, U. S., Geist, E. L., and Andrews, B. D.: Size distribution of submarine landslides and its implication to tsunami hazard in Puerto Rico, Geophys. Res. Lett., 33, L11307, doi:10.1029/2006GL026125, 2006.

Van Den Eeckhaut, M., Poesen, J., Verstraeten, G., Van Acker, V., Nyssen, J., Moeyersons, J., Van Beek, L. P. H., and Vandekerckhove, L.: The use of LIDAR-derived images for mapping old landslides under forest, Earth Surf. Proc. Land., 32, 754–769, 2007.

Whitworth, M., Giles, D., and Murphy, W.: Identification of landslides in clay terrains using Airborne Thematic Mapper (ATM) multispectral imagery, in: Proceedings of the 8th International Symposium on Remote Sensing, SPIE Vol. 4545, 216–224, 2001.

Whitworth, M. C. Z., Gibson, A. D., Forster, A. F., Giles, D. P., Poulton, C., Rowlands, K., and Jones, L. J.: The use of terrestrial laser scanning and digital terrain models for landslide hazard assessment, in: Proceedings of the Annual Conference of the International Association for Mathematical Geology: Predictive Modelling of Geotechnical/Landslide Hazards, University of Portsmouth, Portsmouth, UK, 245, 1–12, 2003.

Whitworth, M. C. Z., Giles, D. P., and Murphy, W.: Airborne remote sensing for landslide hazard assessment: a case study on the Jurassic escarpment slopes of Worcestershire, United Kingdom, Q. J. Eng. Geol. Hydroge., 38, 285–300, 2005.